Available free online at www.medjchem.com

Mediterranean Journal of Chemistry

Mediterranean Journal of Chemistry **2020**, 10(5), 492-501

Physicochemical and in vitro bioactivity studies of bioactive glasses in the SiO_2-CaO-MgO-P_2O_5, SiO_2-Na_2O-CaO-P_2O_5 and SiO_2-Na_2O-CaO-MgO-P_2O_5 systems

Smaiel Herradi, Sara Bouhazma, Imane Adouar, Sanae Chajri, Souad Rakib, Mohamed Khaldi, Brahim El Bali and Mohammed Lachkar *

Engineering Laboratory of Organometallic, Molecular Materials and Environment, Faculty of Sciences, University Sidi Mohammed Ben Abdellah, 30000 Fez, Morocco

Abstract: Glasses in the quaternary and quinary system SiO_2-CaO-MgO-P_2O_5 (SCMP), SiO_2-Na_2O-CaO-P_2O_5 (SNCP) and SiO_2-Na_2O-CaO-MgO-P_2O_5 (SNCMP), have been prepared by using the sol-gel technique. Investigations of structural and bioactive properties of these glasses have been undertaken by using X-ray diffraction (XRD), Fourier Transform Infrared Spectroscopy (FTIR), Scanning Electron Microscopy (SEM) and Energy Dispersive X-ray Spectroscopy (EDS). The *in vitro* bioactivity was assessed by determining the changes in surface morphology and composition after soaking in simulated body fluid (SBF) for up to 30 days at 37°C. X-ray diffraction patterns indicated the formation of hydroxycarbonated apatite layer (HCA) after only one hour for SNCMP glass and after four days for SCMP and SNCP glasses. Furthermore, observed bands of FTIR spectra confirmed the growth of HCA layer during in vitro test.

Moreover, the dissolution rate has been investigated using energy-dispersive X-ray spectroscopy. The observed EDS patterns confirmed the growth of HCA layer on all samples surfaces during *in vitro* analysis. On the one hand, we report the existence of $Na_2Ca_2Si_3O_9$ (that couple good mechanical strength with satisfactory biodegradability) as a single crystalline phase in the SNCP glass when calcined at 600°C. On the other hand, we have noticed that the coexistence of magnesium and sodium both enhanced the dissolution rate and hindered the crystallization in the SNCMP glass at 600°C.

Keywords: Sol-gel; bioactive glasses; sodium; magnesium; in vitro bioactivity.

1. Introduction

In the past, the research for implantable biomaterials was primarily focused on as inert as possible materials that did not interact with the biological environment. Still, this concept was changed with the invention of the first bioactive glass, currently marketed under the name of 45S5 Bioglass® (46.1SiO_2, 24.4Na_2O, 26.9CaO, 2.6P_2O_5 mol.%), by Hench *et al.* in the early 1970s [1]. Since then, numerous studies have focused on bioactive glasses for bone tissue repair due to their ability to bond to living tissues and to stimulate new tissue growth while dissolving over time: these properties make them valuable candidate materials for tissue engineering applications [2]. A common characteristic of bioactive materials is the formation of a calcium phosphate-rich layer on their surface once in contact with physiologic fluids [3,4]. Initially formed amorphous calcium phosphate crystallizes to hydroxycarbonated apatite (HCA), which is analogous to that present in bone. The HCA crystals, reinforced by collagen fibers, form the bonding layer between the bioactive material and the living tissues [5]. Compared with the melt-derived glasses, sol-gel processing allows better control of their bioactive properties by accurate control of their composition and their microstructure [6]. In particular, the lower processing temperature (600°C) permits better control of the glass purity. Moreover, the nanometer scale porosity in the sol-gel glasses offers better control of the dissolution rate after implantation [7]. The traditional bioactive glasses used in biomedical research have a silicate network with the main structure formed by $(SiO_4)^{4-}$ tetrahedra units linked by bridging corners. Due to their low solubility, they are used as long-term implants to replace hard or soft tissues [8]. In addition to SiO_2, various amounts of other oxides may be incorporated into the glass composition to provide peculiar properties to the material; for example, Na_2O, K_2O, CaO and MgO are useful to adjust the surface reactivity in biological environment [9,10]. It was reported that ionic dissolution products from

*Corresponding author: Mohammed Lachkar
Email address: lachkar.mohammed@gmail.com
DOI: http://dx.doi.org/10.13171/mjc10502005161413ml

Received March 21, 2020
Accepted April 12, 2020
Published May 16, 2020

bioactive glasses (e.g. Si, Ca, and P), and from other silicate-based glasses, stimulate expression of several genes of osteoblastic cells [10]. Silicon is known to be an essential element for metabolic processes associated with the formation and calcification of bone tissue [11,12]. High Si contents have been detected in early stages of bone matrix calcification, whereby aqueous Si was shown to be able to induce precipitation of hydroxyapatite. Calcium has a direct role in osteogenesis by stimulating the expression of osteopontin and osteocalcin [9,10]. Magnesium is essential to bone metabolism, and it has been shown to have stimulating effects on new bone formation [13]. It plays a significant role in stimulating osteoblastic cells, and it reduces bone resorption [14]. In this regard, magnesium-contained bioactive glasses are widely studied [3,14,15]. It was found that the incorporation of MgO in the bioactive glass accelerates the early stages of the precipitation of HAC layer [15]. However, some studies have reported that MgO slows down the precipitation rate of HAC [16,17]. Tabia *et al.* have shown that there is no crystallization of HAC layer when magnesium attaint 10 mol % in the ternary bioactive glass $85SiO_2$-(15-x)CaO-xMgO (where x = 0, 1, 3, 5 and 10) [16].

Although bioactive glasses have been used clinically as bone regenerative materials in dental and orthopedic applications [18], these materials usually are very brittle and prone to crack propagation leading to catastrophic failure [19]. Hence, due to their limited mechanical properties, they cannot be used as a bulk material in load-bearing applications [19]. Therefore, the inclusion of sodium in the glass network during the preparation and subsequent thermal treatment are good options for enhancing its mechanical properties through the formation of the crystalline phase $Na_2Ca_2Si_3O_9$ that couples' good mechanical strength with satisfactory biodegradability (the $Na_2Ca_2Si_3O_9$ phase decomposes and transits to amorphous hydroxyapatite (HA), an easily degradable mineral in vivo) [20-22].

The present work deals with the synthesis, *via* a sol-gel route, of three new bioactive glasses compositions, i.e. 60%SiO_2-30%CaO-5%MgO-5% P_2O_5 (SCMP), 64%SiO_2-20%Na_2O-10%CaO-6% P_2O_5 (SNCP) and 60%SiO_2-10%Na_2O-20%CaO-5% MgO-5%P_2O_5 (SNCMP). Effect of addition of sodium and magnesium both in bioactivity and in thermal stability of these glasses is discussed. To our knowledge, this is the first work that studies the effect of magnesium and sodium on the bioactive glasses at the same time.

2. Experimental

2.1. Materials

The following chemicals were used as precursors for the synthesis of the sol-gel glasses, i.e. SCMP, SNCP and SNCMP: tetraethylorthosilicate: $C_8H_{20}O_4Si$ (TEOS) (Aldrich, 99%), triethylphosphate: $C_6H_{15}O_4P$ (TEP) (Eastman, 99.8%), sodium nitrate: $NaNO_3$ (Aldrich, 99%), magnesium nitrate hexahydrate: $Mg(NO_3)_2.6H_2O$ (Loba Chemie, 98%), calcium nitrate tetrahydrate: $Ca(NO_3)_2.4H_2O$ (Loba Chemie, 98%).

2.2. Preparation of bioactive glasses

The exact nominal compositions and the flow chart of the procedure used to generate the three bioactive glasses are given in Table 1 and Scheme 1, respectively. In brief, the molar ratios of TEOS, TEP, $NaNO_3$, $Mg(NO_3)_2.6H_2O$ and $Ca(NO_3)_2.4H_2O$ were designed according to the molar ratio of SiO_2, P_2O_5, CaO, MgO and Na_2O in SCMP, SNCP and SNCMP glasses. To achieve a transparent sol, we used 2N of HNO_3 to catalyse the TEOS and TEP hydrolysis, using a molar ratio of H_2O/(TEOS + TEP) = 8. TEOS, deionized water, and nitric acid were successively mixed, and the mixture was allowed to react for 1h under continuous stirring. Then the appropriate amount of each of the remaining reagents was added and allowed to react entirely for 30 min in the following sequence: (TEP), $Ca(NO_3)_2.4H_2O$, $NaNO_3$ and/or $Mg(NO_3)_2.6H_2O$. After the addition of the last reagent, the mixture was stirred for one additional hour to ensure homogeneity. Next, the solution was introduced in a closed container, where it was allowed to gel at 25°C for 3 d and then was aged at 80°C for 3 d. Then, the aged gel was dried at 150°C for 52 h (gelation, aging and drying of samples were conducted in a programmable oven). The obtained dry gels were ground using an agate mortar. Subsequently, the stabilization of the powders was carried out in an electric furnace at 600°C for 4 h. Finally, these powders were ground again to break down the agglomerates and to enhance the reactivity.

Table 1. Nominal composition (mol %) of the sol-gel glasses.

Sample	SiO_2	CaO	P_2O_5	Na_2O	MgO
SCMP	60	30	5	0	5
SNCP	64	10	6	20	0
SNCMP	60	20	5	10	5

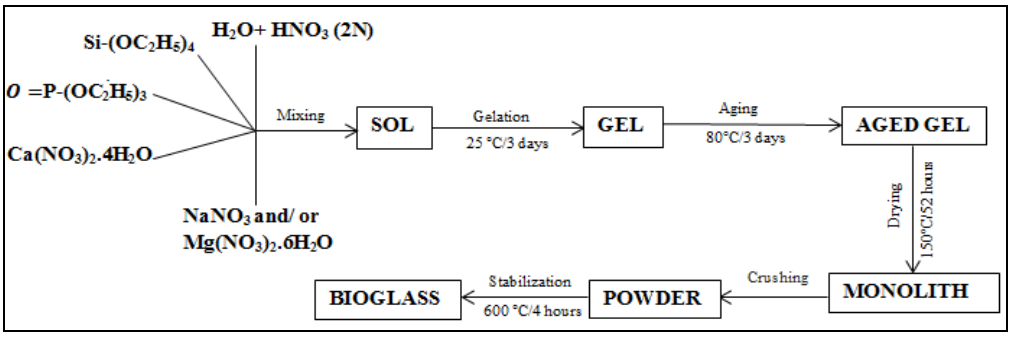

Scheme 1. Procedure used to generate the bioactive glasses SCMP, SNCP and SNCMP

2.3. In vitro bioactivity study of bioactive glasses

The bioactivity of the prepared bioactive glass samples was examined through *in vitro* test where the Simulated Body Fluid (SBF) was prepared according to the method described by Kokubo and Takadama [23]. The test was performed in a polyethylene container in which 0.1g of each sample was immersed in 45 mL of SBF solution (pH = 7.4). The container is incubated at 37°C, in a static condition, for periods of 1 h, 4 d, 7 d, 15 d and 30 d. After soaking, the samples were filtered and dried in air.

2.4. pH behaviour

The stages of formation of hydroxycarbonated apatite layer on the surface of the samples were checked by following the pH of the SBF solution immediately after removing the powder from it. The instrument was calibrated each time with standard buffer solutions.

2.5. Characterizations of the bioactive glasses

The bioactive glasses powders, before and after immersion in SBF, were analysed by X-ray diffraction using a Discover model equipped with a monochromatized Cu-Kα radiation (λ= 1.5418 Å). The diffraction patterns were obtained in the 2θ range [20°-70°]. Fourier transform infrared spectroscopy (FTIR: Bruker VERTEX 70 spectrometer) was used to analyze the functional groups of the obtained powders before and after soaking in SBF. The spectra were recorded from 400 to 4000 cm^{-1} at 4 cm^{-1} resolution. The surface morphology of samples was analyzed before and after soaking in SBF (a set of samples was selected) using a scanning electron microscope (SEM) coupled with energy-dispersive spectroscope: ESEM Quanta 200 (FEI Company).

3. Results and discussion

The XRD patterns of the bioactive glasses SCMP, SNCP and SNCMP, before and after soaking in SBF, are provided in Figures 1, 2 and 3, respectively. For SCMP sample, as it can be observed in Figure 1, both before and after soaking in SBF for 1 h the patterns are typical of an amorphous phase, however, after 4 and 7 d of soaking the formation of an apatite layer is confirmed by (002), (211) and (112) plan reflections. After 15 d, the pattern also shows the (111) plan reflection. The continuous growth of a well crystallized apatite layer on the SCMP sample is confirmed by the existence of eight plan reflections namely (111), (002), (211), (112), (310), (222), (213) and (004). Interestingly, the SNCP sample shows different behaviour. As it can be seen in Figure 2, the pattern of this sample before soaking shows peaks related solely to $Na_2Ca_2Si_3O_9$ crystalline phase [20-22]. Moreover, after 1 h in SBF, all peaks of this phase become more prominent. After 4 d of immersion, none of these peaks is observed, and there is only one intense peak, namely (200), related to hydroxyapatite which suggests that the crystalline phase has been converted to amorphous calcium phosphate which is considered as a template for the nucleation of a new crystalline phase, i.e. the hydroxyapatite. The crystallisation continues after 7, 15 and 30 d and new hydroxyapatite peaks emerge, indicating that the conversion progressed with soaking´s time.

The coexistence of sodium and magnesium in SNCMP glass has dual importance since it enhanced bioactivity and hindered the crystallisation of the $Na_2Ca_2Si_3O_9$ phase at 600°C, which would be beneficial for sintering at higher temperature. Arepalli *et al.* reported that bioactive glasses in the system $(46.10-x)\%SiO_2$-26.9%CaO-24.40%Na_2O-x%MgO-2.6%P_2O_5 (where $0 \leq x \leq 3$ mol %) are bioactive and biocompatible both in vitro and in vivo [14,24]. It is well reported that magnesium slows down the crystallization of the apatite layer [16,17], however, in this work we report the formation of an apatite-like phase after 1 h of soaking in SBF as it can be seen in Figure 3. Additionally, the growth of apatite layer continues to occur as it can be observed from the pattern of SNCMP glass after 30 d of immersion in SBF solution.

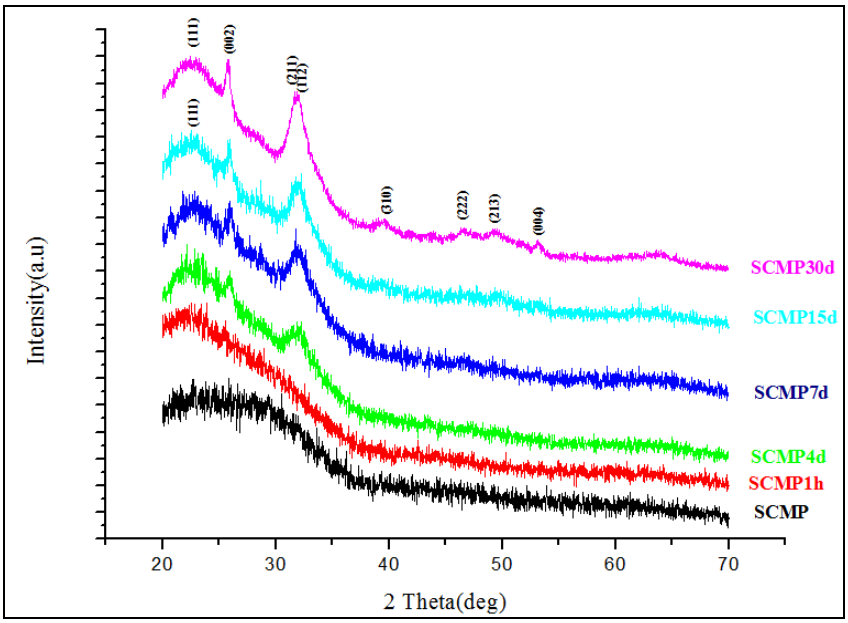

Figure 1. XRD patterns of SCMP glass before and after 1 h, 4, 7, 15 and 30 d soaking in SBF

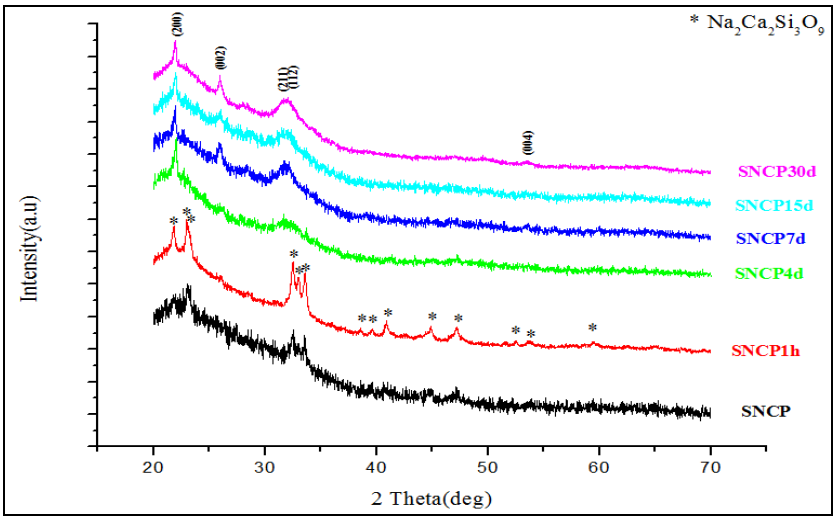

Figure 2. XRD patterns of SNCP glass before and after 1 h, 4, 7, 15 and 30 d soaking in SBF

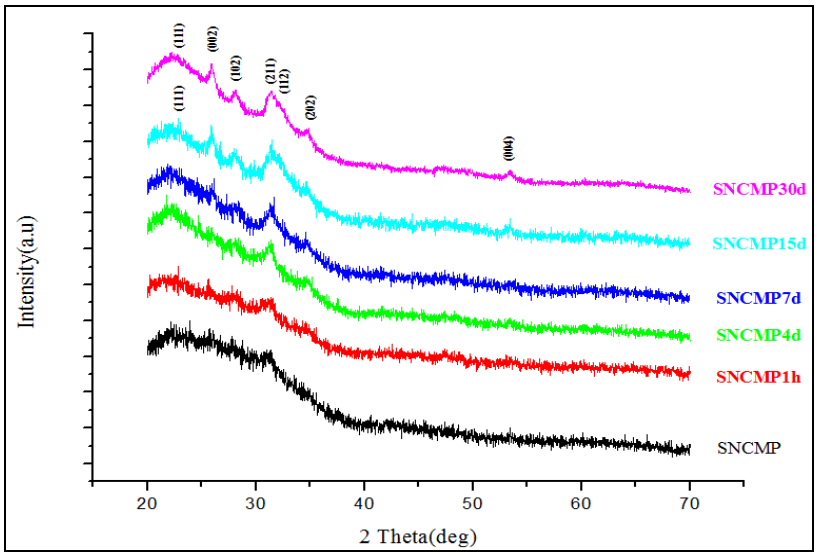

Figure 3. XRD patterns of SNCMP glass before and after 1 h, 4, 7, 15 and 30 d soaking in SBF

The IR spectra of the bioactive glasses SCMP, SNCP and SNCMP, before and after soaking in SBF, are shown in Figures 4, 5 and 6, respectively. The spectra of the as-prepared samples show the absorption bands of the silicate group in the region 1020-1038 cm^{-1}, and at 446 cm^{-1} [25]. In addition, for SNCP and SNCMP glasses, bands at 570 and within 788-794 cm^{-1} are observed and ascribed respectively to the bending vibration mode of P–O in amorphous calcium phosphate and to the symmetric stretching of Si-O-Si bond [25,26]; however, none of these bands is observed for the as-prepared SCMP glass. A broad OH absorption band at 3330 cm^{-1} and a weak adsorbed water band ~ 1635-1660 cm^{-1} appeared in the spectra of as-prepared SCMP and SNCP samples. The band within 1421-1454 cm^{-1} is ascribed to the absorption of carbonate group (ν_3) [20,25]. In contrast, neither water nor carbonate bands were detected for as-prepared SNCMP sample and after 1h in SBF. After 1 h in SBF, no difference is recorded in the spectra of all samples, however, after 4 d in SBF a new absorption band, due to stretching mode of PO_4^{3-} group, is seen within 1029-1035 cm^{-1}.

Interestingly, the vibration band at 570 cm^{-1} (bending mode of P–O) shifted toward 560 cm^{-1} which indicate the formation of a carbonated hydroxyapatite layer [7,25]. The weak band at 868 cm^{-1}, which is recorded only for SCMP glass after 7 d of immersion, is ascribed to C–O bending [25]. As the time of soaking increases, the bands become more and more fine and intense, indicating that the amorphous calcium phosphate is converted continuously into crystalline carbonated hydroxyapatite. The assignments of the observed vibrational frequencies are summarized in Table 2.

Table 2. Assignments of the observed bands in the spectra of samples before and after immersion in SBF.

Assignments	Observed vibrational frequencies (cm^{-1})
Asymmetric stretching vibrational mode of Si–O–Si	1020-1038
Bending mode of Si–O–Si	446
Bending vibration mode of P–O (amorphous)	570
Symmetric stretching vibrational mode of Si–O–Si	788-794
C–O stretching	1421-1454
C–O bending	868
Bending mode of H_2O	1635-1660
O-H stretching (H_2O)	3330
Asymmetric vibration mode of P–O in HA	1029-1035
Bending vibration mode of P–O in HA	560

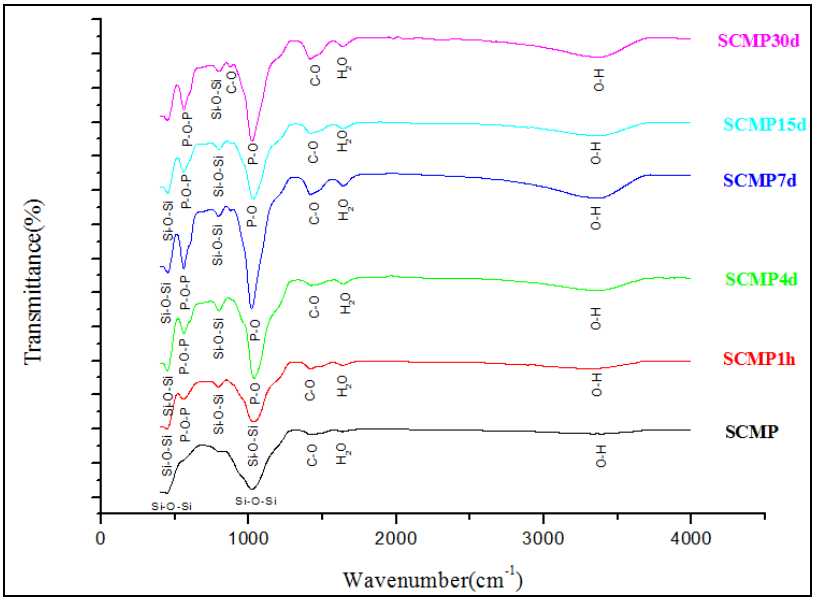

Figure 4. FTIR spectra of SCMP glass before and after 1 h, 4, 7, 15 and 30 d soaking in SBF

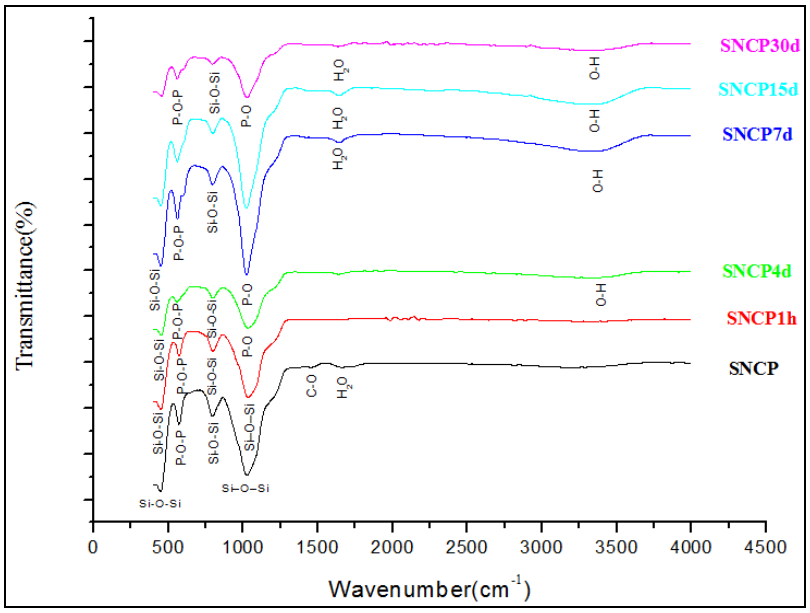

Figure 5. FTIR spectra of SNCP glass before and after 1 h, 4, 7, 15 and 30 d soaking in SBF

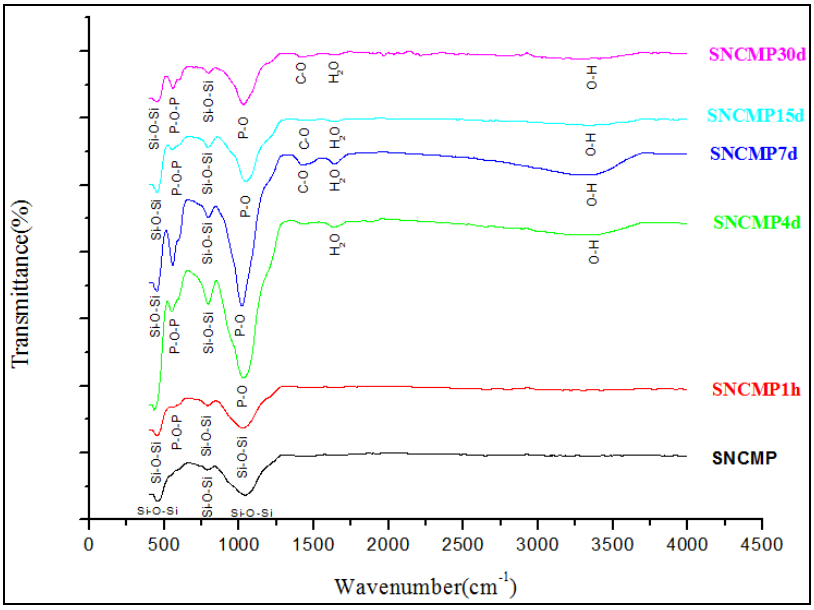

Figure 6. FTIR spectra of SNCMP glass before and after 1 h, 4, 7, 15 and 30 d soaking in SBF

The pH behavior of the SBF solution after immersion of the bioactive glass samples is depicted on Figure 7. After 1 h of soaking, the pH was 8.1 (SCMP) and 7.7 for both SNCP and SNCMP, indicating a high rate dissolution of SCMP compared to SNCP and SNCMP. This might be explained by the fact that in the case of SCMP, there is a fast release of Ca^{2+} ions through the exchange with H_3O^+ ions into the solution. The oxonium ions being replaced with cations, thereby increased hydroxyl concentration of the solution which led to an attack in the silicate glass network and formation of silanols. However, after 4 and 7 d of soaking, the pH for SCMP decreased to 7.78. This might be the result of the migration of Ca^{2+} ions from the solution to form amorphous calcium phosphate where carbonate and magnesium ions could also be incorporated into. After 30 d the respective pH values were 8.1, 8 and 8.2. This behavior may be explained as follow: firstly, rapid ion exchange of Na^+ with H_3O^+ followed by the dissolution of the glass network, polycondensation reaction of surface silanols (Si–OH) to high surface area silica (SiO_2 gel). Secondly, migration of Ca^{2+} and PO_4^{3-} groups to the surface through the SiO_2-rich layer forming a CaO-P_2O_5 rich film on top of the SiO_2-rich layer, followed by a growth of an amorphous CaO-P_2O_5-rich film by incorporation of soluble calcium and phosphate from solution. Thirdly, the crystallization of the amorphous calcium phosphate layer by the inclusion of OH^- and CO_3^{2-} from solution to form HCA layer on the surface of the glass [27]. The dissolution process continues, which leads to a second increase in pH and again to the precipitation of a second HCA layer, and so on. The dissolution process would continue until the consumption of the entire glass network.

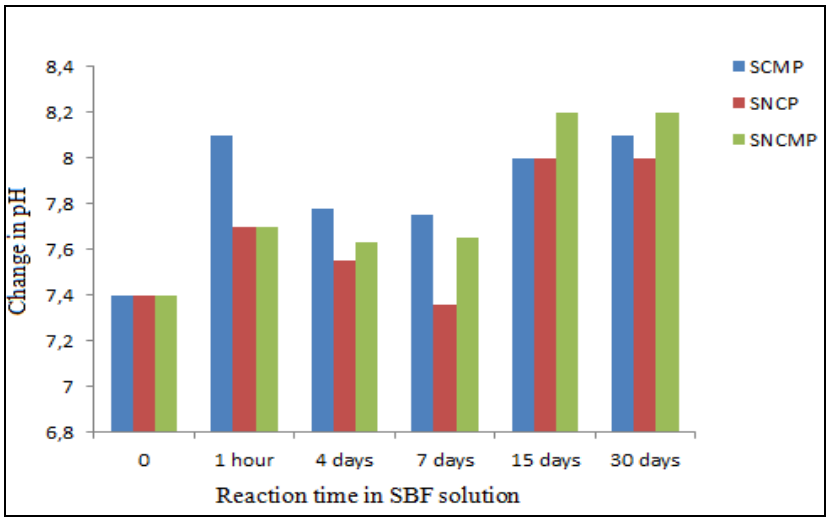

Figure 7. pH of SBF solution before and after soaking of bioactive glasses for 1 h, 4, 7, 15 and 30 d

Figures 8 and 9 show respectively the SEM micrographs and the EDS spectra of SCMP, SNCP and SNCMP sample surfaces before and after soaking in the SBF for 4 and 15 d. After only 4 d, the SEM images show an initial coating of the glasses surfaces with spherical particles.

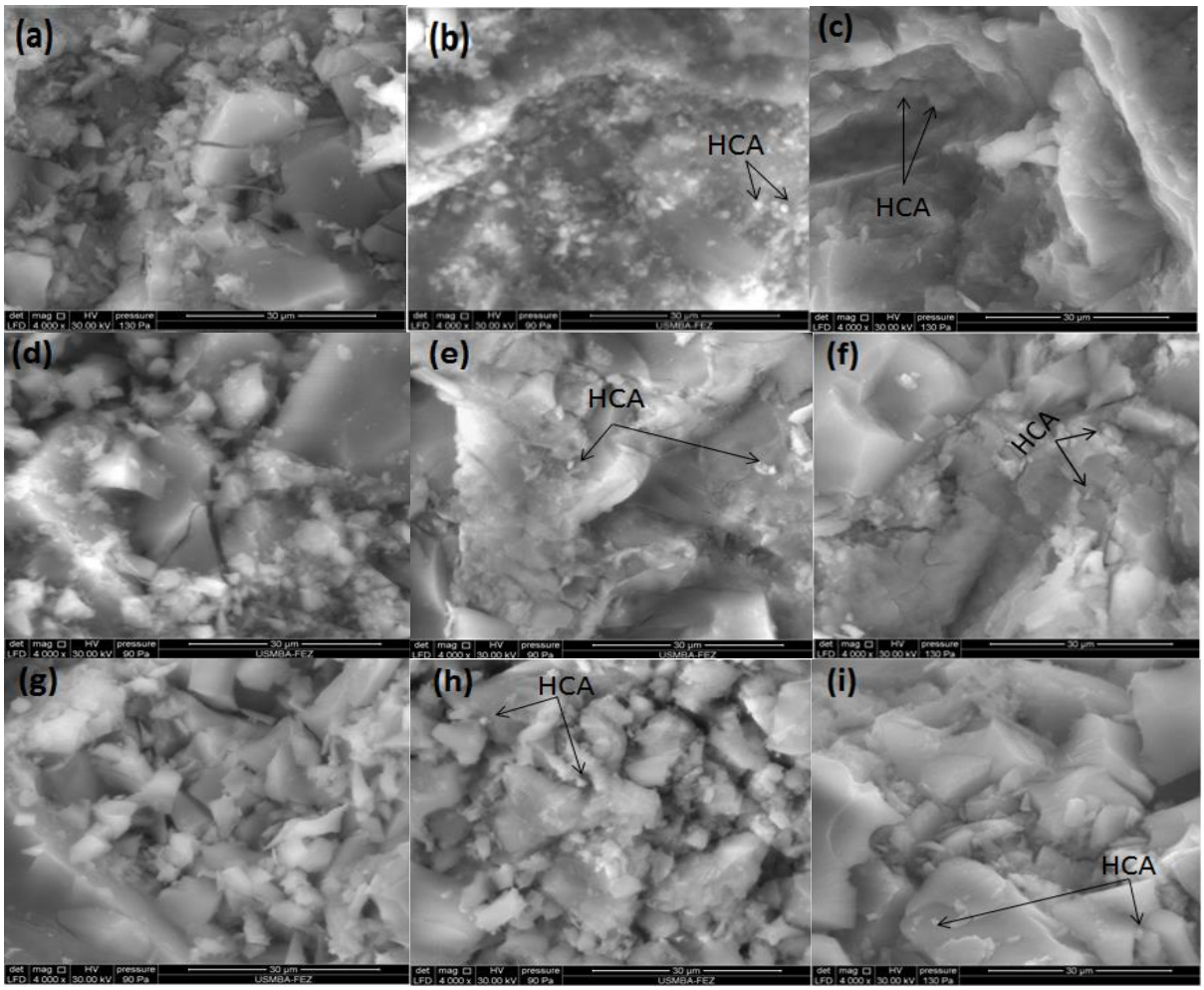

Figure 8. SEM micrographs of the glasses surface before and after soaking in SBF for 4 and 15 d: (a) SCMP (before immersion), (b) SCMP (4 d), (c) SCMP (15 d), (d) SNCP (before immersion), (e) SNCP (4 d), (f) SNCP (15 d), (g) SNCP (before immersion), (h) SNCMP (4 d),(i) SNCMP (15 d)

This growth phenomenon is general; even it is a bit more pronounced in the case of SCMP. It may be because magnesium and sodium are modifiers; as a result, the solubility of the SNCMP glass will be higher than SCMP. The existence of the biodegradable $Na_2Ca_2Si_3O_9$ crystalline phase in the SNCP glass would increase the solubility.

Moreover, the leaching of ions is reported to be one of the reasons to slow down the rate of apatite layer [28]. EDS confirmed the presence of all elements concerning the initial composition of the sol-gell glasses. The surface of the samples after 15 d in SBF showed a different morphology; the newly formed layer cover the glasses surfaces (the most covered one is SCMP glass). The EDS analysis of samples after 15 d in SBF show a remarkable decrease in Si and O concentration and a small decrease in the other initial element, indicating that the dissolution-precipitation processes are in progress, which confirms the previously reported evolution of the pH, and the fact that the newly formed layer is HCA.

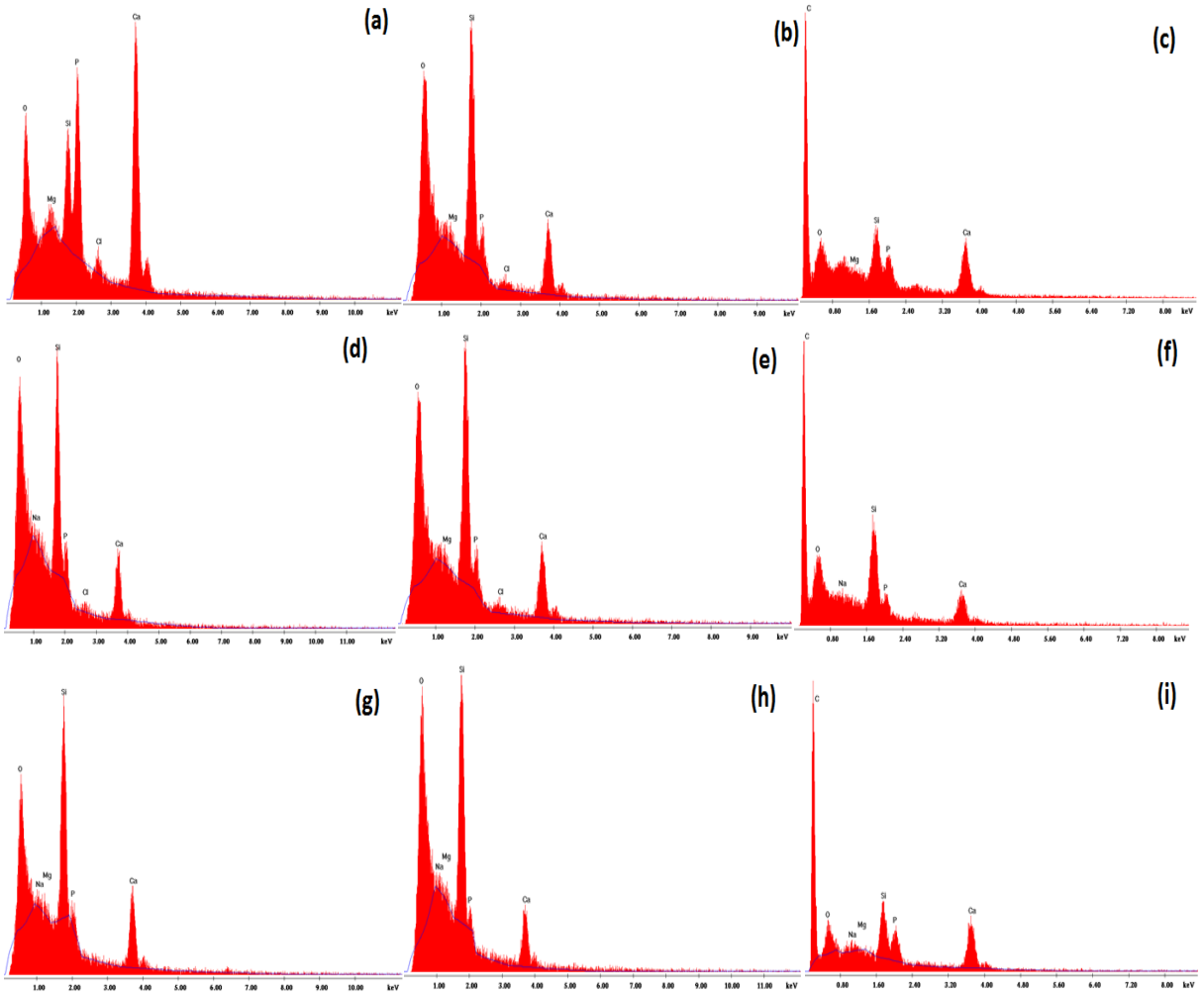

Figure 9. EDS patterns of the glasses surface before and after soaking in SBF for 4 and 15 d: (a) SCMP (before immersion), (b) SCMP (4 d), (c) SCMP (15 d), (d) SNCP (before immersion), (e) SNCP (4 d), (f) SNCP (15 d), (g) SNCP (before immersion), (h) SNCMP (4 d),(i) SNCMP (15 d)

4. Conclusion

In this work, bioactive glasses powders in SiO_2-CaO-MgO-P_2O_5, SiO_2-Na_2O-CaO-P_2O_5 and SiO_2-Na_2O-CaO-MgO-P_2O_5 systems were obtained by a sol-gel technique. The X-ray diffraction patterns, the FTIR spectrum, the pH behavior and the SEM-EDS analyses show that all the synthesized glasses were bioactive. Furthermore, the SNCP glass possesses solely $Na_2Ca_2Si_3O_9$ crystalline phase that converts into HCA layer after only 4 d in SBF. The inclusion of magnesium and sodium at the same time in the glass network has a dual effect since, on the one hand; it inhibits the formation of $Na_2Ca_2Si_3O_9$ crystalline phase and, on the other hand, enhances the in vitro bioactivity of the SNCMP glass. Our outlooks are the optimization of SNCMP glass composition and the realization of in vitro tests in dynamic conditions.

Acknowledgements

The authors would like to acknowledge the support and technical assistance of Interface Regional

University Center (University Sidi Mohammed Ben Abdellah, Fez, Morocco).

References

1- Y. Al-Hadeethi, M. S. Al-Buriahi, M. I. Sayyed, Bioactive glasses and the impact of Si_3N_4 doping on the photon attenuation up to radiotherapy energies, Ceram. Int., **2020**, 46, 5306-5314.
2- F. Baino, G. Novajra, V. Miguez-Pacheco, A. R. Boccaccini, C. Vitale-Brovarone, Bioactive glasses: special applications outside the skeletal system, J. Non-Cryst. Solids, **2016**, 432, 15-30.
3- J. M. Tainio, D. A. Salazar, A. Nommeots-Nomm, C. Roiland, B. Bureau, D. R. Neuville, D.S. Brauerb, J. Massera, Structure and in vitro dissolution of Mg and Sr containing borosilicate bioactive glasses for bone tissue engineering, J. Non-Cryst. Solids, **2020**, 533, 119893.
4- M. Fábián, Z. Kovács, J. L. Lábár, A. Sulyok, Z. E. Horváth, I. Székács, V. K. Kis, Network structure and thermal properties of bioactive (SiO_2-CaO-Na_2O-P_2O_5) glasses, J. Mater. Sci., **2020**, 55, 2303-2320.
5- V. Lalzawmliana, A. Anand, M. Roy, B. Kundu, S. K. Nandi, Mesoporous bioactive glasses for bone healing and biomolecules delivery, Mater. Sci. Eng. C, **2020**, 106, 110180.
6- E. Fiume, C. Migneco, E. Verné, F. Baino, Comparison between Bioactive Sol-Gel and Melt-Derived Glasses/Glass-Ceramics Based on the Multicomponent SiO_2-P_2O_5-CaO-MgO-Na_2O-K_2O System, Materials, **2020**, 13, 540.
7- N. Ranga, S. Gahlyan, S. Duhan, Antibacterial Efficiency of Zn, Mg and Sr Doped Bioactive Glass for Bone Tissue Engineering, J. Nanosci. Nanotechnol., **2020**, 20, 2465-2472.
8- H. E. Skallevold, D. Rokaya, Z. Khurshid, M. S. Zafar, Bioactive Glass Applications in Dentistry, Int. J. Mol. Sci., **2019**, 20, 5960.
9- P. K. Modi, A. Prabhu, Y. P. Bhandary, S. Shenoy, A. Hegde, S. P. ES, R. P. Johnson, S. P. Das, S. Vazirally, P. D. Rekha, Effect of calcium glucoheptonate on proliferation and osteogenesis of osteoblast-like cells in vitro, PloS one, **2019**, 14, e0222240.
10- P. Naruphontjirakul, O. Tsigkou, S. Li, A. E. Porter, J. R. Jones, Human mesenchymal stem cells differentiate into an osteogenic lineage in the presence of strontium containing bioactive glass nanoparticles, Acta biomater., **2019**, 90, 373-392.
11- S. K. Venkatraman, S. Swamiappan, Review on calcium and magnesium-based silicates for bone tissue engineering applications, J. Biomed. Mater. Res. A, **2020**,108, 1546-1562.
12- W. Götz, E. Tobiasch, S. Witzleben, M. Schulze, Effects of silicon compounds on biomineralization, osteogenesis, and hard tissue formation, Pharmaceutics, **2019**, 11, 117.
13- M. M. Belluci, R. S. de Molon, C. Rossa Jr, S. Tetradis, G. Giro, P. S. Cerri, E. Marcantonio Jr, S. R. P. Orrico, Severe magnesium deficiency compromises systemic bone mineral density and aggravates inflammatory bone resorption, J. Nutr. Biochem., **2020**, 77, 108301.
14- S. K. Arepalli, H. Tripathi, P. P. Manna, P. Pankaj, S. Krishnamurthy, S. C. Patne, R. Pyare, S. P. Singh, Preparation and in vitro investigation on the bioactivity of magnesia-contained bioactive glasses, J. Aust. Ceram. Soc., **2019**, 55, 145-155.
15- B. Karakuzu-Ikizler, P. Terzioğlu, Y. Basaran-Elalmis, B. S. Tekerek, S. Yücel, Role of magnesium and aluminum substitution on the structural properties and bioactivity of bioglasses synthesized from biogenic silica, Bioact. Mater., **2020**, 5, 66-73.
16- Z. Tabia, K. El Mabrouk, M. Bricha, K. Nouneh, Mesoporous bioactive glass nanoparticles doped with magnesium: drug delivery and acellular in vitro bioactivity, RSC Adv., **2019**, 9, 12232-12246.
17- A. Moghanian, A. Sedghi, A. Ghorbanoghli, E. Salari, The effect of magnesium content on in vitro bioactivity, biological behavior and antibacterial activity of sol-gel derived 58S bioactive glass, Ceram. Int., **2018**, 44, 9422-9432.
18- W. Hong, Q. Zhang, H. Jin, L. Song, Y. Tan, L. Luo, F. Guo, X. Zhao, P. Xiao, Roles of strontium and hierarchy structure on the in vitro biological response and drug release mechanism of the strontium-substituted bioactive glass microspheres, Mater. Sci. Eng., C, **2020**, 107, 110336.
19- M. S. Zafar, I. Farooq, M. Awais, S. Najeeb, Z. Khurshid, S. Zohaib, In Biomedical, therapeutic and clinical applications of bioactive glasses; ed. by G. Kaur; Woodhead Publishing: Cambridge, UK, **2019**, 313-329.
20- A. Thomas, E. Johnson, A. K. Agrawal, J. Bera, Preparation and characterization of glass-ceramic reinforced alginate scaffolds for bone tissue engineering, J. Mater. Res., **2019**, 34, 3798-3809.
21- C. Blaeß, R. Müller, G. Poologasundarampillai, D. S. Brauer, Sintering and concomitant crystallization of bioactive glasses, Int. J. Appl. Glass Sci., **2019**, 10, 449-462.
22- E. N. Bulanov, M. S. Boldin, A. V. Knyazev, V. Z. Korokin, A. A. Popov, Obtaining Ceramic Materials from Hydroxyapatite Using Spark-Plasma Sintering, High Temp. Mater. Processes, **2018**, 37, 613-617.
23- T. Kokubo, H. Takadama, How useful is SBF in predicting in vivo bone bioactivity? , Biomaterials, **2006**, 27, 2907-2915.
24- S. K. Arepalli, H. Tripathi, P. P. Manna, P. Pankaj, S. Krishnamurthy, S. C. Patne, R. Pyare, S. P. Singh, Enhanced in vivo biocompatibility of magnesia-contained bioactive glasses, J. Aust. Ceram. Soc., **2019**, 55, 337-342.

25- R. Karan, P. Manna, P. K. Maiti, K. Das, Influence of selenium dioxide (SeO_2) on properties of bioglass in SiO_2-Na_2O-CaO-P_2O_5 system, J. Aust. Ceram. Soc., **2020**, 1-11.
26- S. Chajri, S. Bouhazma, I. Adouar, S. Herradi, M. Khaldi, B. El Bali, M. Lachkar, Synthesis, characterization and evaluation of bioactivity of glasses in the CaO-SiO_2-P_2O_5-MgO system with different CaO/MgO ratios, J. Phys. Conf. Ser., **2019**, 1292, 012013.
27- A. Bachar, R. Catteaux, C. Duée, F. Désanglois, I. Lebecq, C. Mercier, C. Follet-Houttemane, In Biomedical, therapeutic and clinical applications of bioactive glasses; ed. by G. Kaur; Wood head Publishing: Cambridge, UK, **2019**, 69-123.
28- H. R. Fernandes, A. Gaddam, A. Rebelo, D. Brazete, G. E. Stan, J. M. Ferreira, Bioactive glasses and glass-ceramics for healthcare applications in bone regeneration and tissue engineering, Materials, **2018**, 11, 2530.